Second-Order Statistics of κ−μ Shadowed Fading Channels

Cotton, S. L. (2016). Second-Order Statistics of κ−μ Shadowed Fading Channels. *IEEE Transactions on Vehicular Technology*, *65*(10), 8715 - 8720. https://doi.org/10.1109/TVT.2015.2506260

Published in:
IEEE Transactions on Vehicular Technology

Document Version:
Publisher's PDF, also known as Version of record

where $A=\int_1^{e^{\mathcal{I}_L^A}}\int_1^{\psi_1}\cdots\int_1^{\alpha}D[-\ln(\psi_{L-1}-1)](1/\psi_{L-1})d\psi_{L-1}\prod(1/\psi_i)d\psi_i$, and $B=\int_1^{e^{\mathcal{I}_L^A}}\int_1^{\psi_1}\cdots\int_1^{\alpha}D[\ln(\rho)-C](1/(\psi_{L-1}))d\psi_{L-1}\prod(1/\psi_i)d\psi_i$. If we set $y=\psi_{L-1}-1$, then $A=\int_1^{e^{\mathcal{I}_L^A}}\int_1^{\psi_1}\cdots\int_0^{\alpha-1}D[-\ln(y)](1/(y+1))dy\prod(1/\psi_i)d\psi_i$. From [15, eq. (4.231)], we know that $\int_0^0(\ln(x)/(1+x))dx=(-\pi^2)/12$ is finite compared with $\ln(\rho)-C$. Therefore, A is finite compared with B. Then, P_1 can be approximated as $e^{\mathcal{I}_L^A}(\prod_{i=1}^{L}(1/i\rho\eta))[\ln(\rho)-C]B$. Finally, we get the approximation of P_1 as $P_1\approx e^{\mathcal{I}_L^A}(\prod_{i=1}^{L}(1/i\rho\eta))[\ln(\rho)-C]^2\int_1^{e^{\mathcal{I}_L^A}}\int_1^{\psi_1}\cdots\int_1^{\alpha}D\prod_{i=1}^{L-1}(1/\psi_i)d\psi_i$. With similar steps and some simple steps, we can approximate the pdf of $\mathcal{I}_L^A$ as $f_L(\mathcal{I}_L^A)\approx e^{\mathcal{I}_L^A}(([\ln(\rho)-C]^L(\mathcal{I}_L^A)^{L-1})/(\rho\eta)^L L!(L-1)!)$. Therefore, at high SNR, $P(\mathcal{O}_L)=\int_0^{LR(L)}f_L(\mathcal{I}_L^A)d\mathcal{I}_L^A\approx(([\ln(\rho)-C]^L)/(\rho\eta)^L L!(L-1)!)\int_0^{LR(L)}e^{\mathcal{I}_L^A}(\mathcal{I}_L^A)^{L-1}d\mathcal{I}_L^A$. Applying [15, eq. (2.321)], $\int x^n e^{ax}dx=e^{ax}(\sum_{k=0}^{n}(((-1)^k k!\binom{n}{k}))/(a^{k+1})x^{n-k}))$. Then, the theorem is proved. ■

APPENDIX D
PROOF OF COROLLARY 5

From Section III, we know that $P(\mathcal{O})=\sum_{L=0}^{M}P(L)P(\mathcal{O}_L)$. Moreover, based on the expression of $P(\mathcal{O}_L)$ at high SNR (11), we can get $P(\mathcal{O}_L)\doteq\rho^{-L}$, where $\doteq$ denotes the exponential equality (i.e., $f(\rho)\doteq\rho^n$ means $-\lim_{\rho\to\infty}(\ln f(\rho)/\ln(\rho))=n$) [11]. On the other hand, $P(L)=(M!/L!)e^{-L\varepsilon(L)}T(L+1)\doteq T(L+1)$. $T(L)=\int_0^{\varepsilon(M)}\int_{x_M}^{\varepsilon(M-1)}\cdots\int_{x_{L+2}}^{\varepsilon(L+1)}\int_{x_{L+1}}^{\varepsilon(L)}\prod_{i=L}^{M}e^{-x_i}dx_i\doteq\int_0^{\varepsilon(M)}\int_{x_M}^{\varepsilon(M-1)}\cdots\int_{x_{L+2}}^{\varepsilon(L+1)}\int_{x_{L+1}}^{\varepsilon(L)}\prod_{i=L}^{M}dx_i$. After calculating the integrals of x_i $(L\le i\le M)$, we get $T(L)\doteq(((-1)^{M-L})/(M-L+1)!)\,\varepsilon(M)^{M-L+1}+\sum_{i=1}^{M-L}(((-1)^{i-1})/i!)\varepsilon(L+i-1)^i T(L+i)$. Since $\varepsilon(i)\doteq\rho^{-1}(1\le i\le M)$ and $T(M)\doteq\int_0^{\varepsilon(M)}dx_M=\varepsilon(M)\doteq\rho^{-1}$, we know $T(L)\doteq\rho^{-(M-L+1)}$. By combining the truth $P(L)\doteq T(L+1)$, we can obtain $P(L)\doteq\rho^{-(M-L)}$. Then, the corollary is proved. ■

REFERENCES

[1] R. Zhang and C. K. Ho, "MIMO broadcasting for simultaneous wireless information and power transfer," *IEEE Trans. Wireless Commun.*, vol. 12, no. 5, pp. 1989–2001, May 2013.

[2] A. A. Nasir, X. Zhou, S. Durrani, and R. A. Kennedy, "Relaying protocols for wireless energy harvesting and information processing," *IEEE Trans. Wireless Commun.*, vol. 12, no. 7, pp. 3622–3636, Jul. 2013.

[3] I. Krikidis, "Simultaneous information and energy transfer in large-scale networks with/without relaying," *IEEE Trans. Signal Process.*, vol. 63, no. 7, pp. 1700–1711, Mar. 2015.

[4] D. Michalopoulos, H. Suraweera, and R. Schober, "Relay selection for simultaneous information transmission and wireless energy transfer: A tradeoff perspective," *IEEE Signal Process. Lett.*, vol. 21, no. 4, pp. 454–458, Aug. 2014.

[5] P. Xu, X. Dai, Z. Ding, I. Krikidis, and K. K. Leung, "Approaching MISO upper bound: Design of new wireless cooperative transmission protocols," *IEEE Trans. Wireless Commun.*, vol. 10, no. 8, pp. 2725–2737, Aug. 2011.

[6] S. Yang and J.-C. Belfiore, "Towards the optimal amplify-and-forward cooperative diversity scheme," *IEEE Trans. Inf. Theory.*, vol. 53, no. 9, pp. 3114–3126, Sep. 2007.

[7] A. Bletsas, A. Khisti, D. P. Reed, and A. Lippman, "A simple cooperative diversity method based on network path selection," *IEEE J. Sel. Areas Commun.*, vol. 24, no. 3, pp. 659–672, Mar. 2006.

[8] J. K. Tugnait and W. Luo, "On channel estimation using superimposed training and first-order statistics," *IEEE Commun. Lett.*, vol. 7, no. 9, pp. 417–431, Sep. 2003.

[9] Z. Ding, T. Ratnarajah, and C. F. Cowan, "HOS-based semi-blind spatial equalization for MIMO Rayleigh fading channels," *IEEE Trans. Signal Process.*, vol. 56, no. 1, pp. 248–255, Jan. 2008.

[10] Z. Ding, S. M. Perlaza, I. Esnaola, and H. V. Poor, "Power allocation strategies in energy harvesting wireless cooperative networks," *IEEE Trans. Wireless Commun.*, vol. 13, no. 2, pp. 846–860, Feb. 2014.

[11] L. Zheng and D. N. C. Tse, "Diversity and multiplexing: A fundamental tradeoff in multiple-antenna channels," *IEEE Trans. Inf. Theory.*, vol. 49, no. 5, pp. 1073–1096, May 2003.

[12] H. A. David and H. N. Nagaraja, *Order Statistics*. Hoboken, NJ, USA: Wiley, 1970.

[13] T. Ratnarajah and R. Vaillancourt, "Quadratic forms on complex random matrices and multiple-antenna systems," *IEEE Trans. Inf. Theory.*, vol. 51, no. 8, pp. 2976–2984, Aug. 2005.

[14] Z. Ding, T. Ratnarajah, and C. C. Cowan, "On the diversity-multiplexing tradeoff for wireless cooperative multiple access systems," *IEEE Trans. Signal Process.*, vol. 55, no. 9, pp. 4627–4638, Sep. 2007.

[15] I. S. Gradshteyn and I. M. Ryzhik, *Table of Integrals, Series and Products*, 6th ed. San Diego, CA, USA: Academic, 2000.

Second-Order Statistics of $\kappa-\mu$ Shadowed Fading Channels

Simon L. Cotton, *Senior Member, IEEE*

***Abstract*—In this paper, novel closed-form expressions for the level crossing rate and average fade duration of $\kappa-\mu$ shadowed fading channels are derived. The new equations provide the capability of modeling the correlation between the time derivative of the shadowed dominant and multipath components of the $\kappa-\mu$ shadowed fading envelope. Verification of the new equations is performed by reduction to a number of known special cases. It is shown that as the shadowing of the resultant dominant component decreases, the signal crosses lower threshold levels at a reduced rate. Furthermore, the impact of increasing correlation between the slope of the shadowed dominant and multipath components similarly acts to reduce crossings at lower signal levels. The new expressions for the second-order statistics are also compared with field measurements obtained for cellular device-to-device and body-centric communication channels, which are known to be susceptible to shadowed fading.**

***Index Terms*—Average fade duration (AFD), body-centric communications, device-to-device (D2D) communications, land mobile satellite communications, level crossing rate (LCR), shadowed fading, $\kappa-\mu$ fading channels.**

I. INTRODUCTION

The $\kappa-\mu$ shadowed fading model first appeared in the literature in [1] and immediately after this in [2]. It has been proposed as a generalization of the popular $\kappa-\mu$ fading model [3]. In this model, clusters of multipath waves are assumed to have scattered waves with identical power values, alongside the presence of elective dominant signal components—a scenario that is identical to that observed in $\kappa-\mu$ fading [3]. The key difference between the $\kappa-\mu$ shadowed fading model and that of classical $\kappa-\mu$ fading is that the dominant

Manuscript received July 21, 2014; revised May 29, 2015, August 23, 2015; accepted October 5, 2015. Date of publication December 7, 2015; date of current version October 13, 2016. This work was supported in part by the U.K. Royal Academy of Engineering, by the Engineering and Physical Sciences Research Council under Grant EP/H044191/1 and Grant EP/L026074/1, and by Leverhulme Trust, U.K. under Grant PLP-2011-061. The review of this paper was coordinated by Prof. T. Kuerner.

The author is with the Institute of Electronics, Communications and Information Technology, Queen's University Belfast, Belfast BT7 1NN, U.K. (e-mail: simon.cotton@qub.ac.uk).

Digital Object Identifier 10.1109/TVT.2015.2506260

components of all the clusters can randomly fluctuate because of shadowing. In particular, it is assumed that the shadowing fluctuation follows a Nakagami distribution [4]. Similar to the $\kappa-\mu$ distribution, the $\kappa-\mu$ shadowed distribution is an extremely versatile fading model that also contains, as special cases, other important distributions such as the one-sided Gaussian, Rice (Nakagami-n), Nakagami-m, and Rayleigh distributions. In addition to this, it also contains, as a special case, Abdi's signal reception model [5], which considers Rician fading where the dominant component also undergoes shadowed fading that follows the Nakagami distribution. Due to the ability of the Nakagami probability density function (pdf) to approximate the lognormal pdf [6], the $\kappa-\mu$ shadowed fading model can be also used to estimate Loo's well-known model for land mobile satellite communications [7].

While the research studies on composite fading models, such as the $\kappa-\mu$/gamma model [8] and its associated second-order statistics including the level crossing rate (LCR) and average fade duration (AFD) [9], have advanced, unfortunately, at present, similar closed-form expressions for the second-order statistics of the $\kappa-\mu$ shadowed model are currently unavailable in the literature. The LCR and AFD of a fading signal are of great importance in the design of mobile radio systems and in the analysis of their performance [10]. Among their many potential applications are the design of error-correcting codes, the optimization of interleaver size, and system throughput analysis as well as channel modeling and simulation. In this paper, convenient closed-form expressions for the LCR and AFD of $\kappa-\mu$ shadowed fading channels are derived and subsequently verified by reduction to known special cases. An important empirical validation is also performed through comparison with field measurements from two different types of wireless channel, which are known to suffer from shadowed fading, namely, cellular device-to-device (D2D) communication channels [2] and body-centric communication channels [11].

The remainder of this paper is organized as follows. Section II provides a brief overview of the $\kappa-\mu$ shadowed fading model. Important relationships between the $\kappa-\mu$ shadowed fading envelope and its time derivative, which underlie the second-order equations proposed here, are established in Section III. Also presented in Section III is the derivation of the LCR, whereas the derivation of the AFD is given in Section IV. The new expressions for the LCR and AFD of the $\kappa-\mu$ shadowed fading model are compared with some empirical data obtained from field measurements in Section V. Finally, Section VI finishes this paper with some concluding remarks.

II. Overview of the $\kappa-\mu$ Shadowed Fading Model

The $\kappa-\mu$ shadowed fading model was originally proposed in [1]. A slight variant of the underlying signal model was also independently developed and appeared shortly after this in [2]. In [1], a rigorous mathematical development of the model was performed, whereas in [2], the model was the result of channel measurements conducted to characterize the shadowed fading observed in D2D communication channels. Both papers have developed important statistics related to the $\kappa-\mu$ shadowed fading model such as the pdf and the moment-generating function. In [1], the cumulative distribution function (cdf) and the sum and maximum distributions of independent but arbitrarily distributed $\kappa-\mu$ shadowed variates were also derived, whereas the moments of this model were presented in [2]. In the sequel, the model presented in [1] is used to develop the LCR and AFD equations proposed here. It is worth highlighting that the models proposed in [1] and [2] are related by a simple scaling factor applied to the dominant signal component, and thus, either of the two models could be used to arrive at the second-order equations presented here.

The received signal envelope, i.e., R, of the $\kappa-\mu$ shadowed fading model may be expressed in terms of the in-phase and quadrature components of the fading signal such that [1]

$$R^2=\sum_{i=1}^{\mu}(X_i+\xi p_i)^2+(Y_i+\xi q_i)^2 \tag{1}$$

where μ is the number of multipath clusters, which is initially assumed to be a natural number,[1] and X_i and Y_i are mutually independent Gaussian random processes with mean $E[X_i]=E[Y_i]=0$ and variance $E[X_i^2]=E[Y_i^2]=\sigma^2$ (i.e., the power of the scattered waves in each of the clusters). Here, p_i and q_i are the mean values of the in-phase and quadrature phase components of multipath cluster i, and $d^2=\sum_{i=1}^{\mu}p_i^2+q_i^2$. In this model, all of the dominant components are subject to the same common shadowing fluctuation, i.e., ξ, which is a Nakagami-m random variable with the shaping parameter m used to control the amount of shadowing experienced by the dominant components, and $E[\xi^2]=1$. As with the $\kappa-\mu$ model [3], $\kappa>0$ is simply the ratio of the total power of the dominant components (d^2) to the total power of the scattered waves ($2\mu\sigma^2$), and the mean power is given by $E[R^2]=\bar{r}^2=d^2+2\mu\sigma^2$. While the pdf of R, i.e., $f_R(r)$, could be obtained from [2, eq. (8)] by expressing the mean power of the dominant component (Ω) in terms of κ and $\bar{r}$, that is, $\Omega=\kappa\bar{r}^2/(\kappa+1)$, for the purposes of this derivation, it is obtained from the pdf of the instantaneous signal-to-noise ratio (SNR) (γ) given in [1, eq. (4)] via a transformation of variables ($\gamma=r^2\bar{\gamma}/\bar{r}^2$) as

$$f_R(r)=\frac{2r^{2\mu-1}\mu^{\mu}m^m(1+\kappa)^{\mu}}{\Gamma(\mu)(\mu\kappa+m)^m\bar{r}^{2\mu}} \times\exp\left(-\frac{\mu(1+\kappa)r^2}{\bar{r}^2}\right){}_1F_1\left(m;\mu;\frac{\mu^2\kappa(1+\kappa)}{\mu\kappa+m}\frac{r^2}{\bar{r}^2}\right) \tag{2}$$

where $\Gamma(\bullet)$ is the gamma function, and ${}_1F_1(\bullet;\bullet;\bullet)$ is the confluent hypergeometric function [12]. In this model, m is allowed to take any value in the range $m\geq 0$, where $m=0$ corresponds to complete shadowing of the resultant dominant component, and $m\to\infty$ corresponds to no shadowing of the resultant dominant component. Naturally, when $m=\infty$, the pdf given in (2) becomes equivalent to the $\kappa-\mu$ pdf given in [3], whereas when $m=0$, and hence $\kappa=0$, the pdf given in (2) reduces to the Nakagami pdf [4].

III. Level Crossing Rate

The LCR of a fading signal envelope, i.e., $N_R(r)$, is defined as the expected number of times that the envelope crosses a given signal level in a positive (or negative) direction per second and is given by [13]

$$N_R(r)=\int_0^{\infty}\dot{r}f_{R,\dot{R}}(r,\dot{r})d\dot{r} \tag{3}$$

where $\dot{r}$ is the time derivative of r, and $f_{R,\dot{R}}(r,\dot{r})$ is the joint probability density of R and $\dot{R}$. If we initially hold the shadowing fluctuation constant, the variation of the signal envelope would follow a $\kappa-\mu$ distribution [3]. In this instance, from (1), it is easy to see that the $\kappa-\mu$ signal power can be obtained as the sum of μ squared Rice variates. This is a simple but important observation as it allows us to show that the pdf of the time derivative of R, which is denoted as $\dot{R}$, is zero-mean Gaussian distributed. Letting Z represent a Rice distributed random variable, it follows that:

$$R^2=\sum_{i=1}^{\mu}Z_i^2. \tag{4}$$

[1]Note that this restriction is later relaxed by allowing μ to assume any positive real value.

Differentiating both sides of (4) with respect to time, we find that

$$\dot{R} = \frac{\sum_{i=1}^{\mu} Z_i \dot{Z}_i}{R}. \tag{5}$$

Knowing that for the Rice case, $\dot{Z}$ is a zero-mean Gaussian distributed random variable with variance $\dot{\sigma}_Z^2 = 2\pi^2 f_m^2 \sigma^2$ [14, eq. (2.104)], where f_m is the maximum Doppler frequency, it is straightforward to show that, in fact, $\dot{\sigma}_R^2 \equiv \dot{\sigma}_Z^2$. From [3], $\sigma^2 = \bar{r}^2/2\mu(1+\kappa)$, and therefore

$$\dot{\sigma}_R^2 = \frac{\pi^2 f_m^2 \bar{r}^2}{\mu(1+\kappa)}. \tag{6}$$

Most importantly though, from (5), we can see that $\dot{R}$ is obtained as a linear transformation of $\dot{Z}$, and thus, it can be deduced in a similar fashion to [13] that the pdf of the rate of change of the envelope $\dot{R}$ is uncorrelated with R, and thus, $f_{R,\dot{R}}(r,\dot{r}) = f_R(r) \times f_{\dot{R}}(\dot{r})$.

Now, consider the shadowed fluctuation of the dominant component separately, which, in this model, is assumed to follow a Nakagami-m distribution. Using the model given in [15], it has already been shown that the slope is zero-mean Gaussian distributed and that its pdf is independent of the envelope, and thus, $f_{R,\dot{R}}(r,\dot{r}) = f_R(r) \times f_{\dot{R}}(\dot{r})$. Knowing that the Nakagami-m distribution appears as a special case of the $\kappa-\mu$ distribution, the variance of the slope can be also obtained by letting $\kappa = 0$ in (6), $\mu = m$, and interchanging $\bar{r}^2$ with Ω such that $\dot{\sigma}_R^2 = \pi^2 f_m^2 \Omega/m$. As above, to remove the dependence of the formulations on the mean power of the dominant component, we substitute $\Omega = \kappa\bar{r}^2/(1+\kappa)$, which gives

$$\dot{\sigma}_R^2 = \frac{\pi^2 f_m^2 \kappa \bar{r}^2}{m(1+\kappa)}. \tag{7}$$

Having demonstrated that for both the multipath and shadowing, the variations of the fading components are independent of the pdf of the time derivative of the envelope, it now becomes possible to rewrite (3) as

$$N_R(r) = f_R(r) \int_0^{\infty} \dot{r} f_{\dot{R}}(\dot{r}) d\dot{r} \tag{8}$$

where $f_R(r)$ is the $\kappa-\mu$ shadowed pdf given in (2), and $f_{\dot{R}}(\dot{r})$ is the pdf of the rate of change of the envelope $\dot{R}$. Following the approach taken in [7], it seems reasonable to assume that the pdf of $\dot{R}$ is the result of two correlated zero-mean Gaussian random processes. Letting $\dot{R} = \dot{A} + \dot{B}$, where $\dot{A}$ is the rate of change of the envelope due to the multipath component, and $\dot{B}$ is the rate of change of the envelope due to the shadowed dominant component, the joint density of $\dot{A}$ and $\dot{B}$ is given by [16]

$$f_{\dot{A},\dot{B}}(\dot{a},\dot{b}) = \frac{1}{2\pi\dot{\sigma}_A\dot{\sigma}_B\sqrt{1-\rho^2}} \times \exp\left[-\frac{1}{2(1-\rho^2)}\left(\frac{\dot{a}^2}{\dot{\sigma}_A^2} - \frac{2\rho\dot{a}\dot{b}}{\dot{\sigma}_A\dot{\sigma}_B} + \frac{\dot{b}^2}{\dot{\sigma}_B^2}\right)\right] \tag{9}$$

where $\dot{\sigma}_A^2$ and $\dot{\sigma}_B^2$ are the variances of the two random variables $\dot{A}$ and $\dot{B}$, and ρ is the correlation between them. Substituting $\dot{A} = \dot{R} - \dot{B}$ into (9), the integral $f_{\dot{R}}(\dot{r}) = \int_{-\infty}^{\infty} f_{\dot{A},\dot{B}}(\dot{r}-\dot{b},\dot{b})d\dot{b}$ can be evaluated as [7]

$$f_{\dot{R}}(\dot{r}) = \frac{1}{\left[2\pi(1-\rho^2)\left(\dot{\sigma}_A^2 + 2\rho\dot{\sigma}_A\dot{\sigma}_B + \dot{\sigma}_B^2\right)\right]^{1/2}} \times \exp\left[-\frac{\dot{r}^2}{2(1-\rho^2)\dot{\sigma}_A^2}\left(\frac{\dot{\sigma}_A^2(1-\rho^2) + 4\rho\dot{\sigma}_A\dot{\sigma}_B}{\dot{\sigma}_A^2 + 2\rho\dot{\sigma}_A\dot{\sigma}_B + \dot{\sigma}_B^2}\right)\right] \tag{10}$$

and therefore

$$\int_0^{\infty} \dot{r} f_{\dot{R}}(\dot{r}) d\dot{r} = \frac{\sqrt{(1-\rho^2)\left(\dot{\sigma}_A^2 + 2\rho\dot{\sigma}_A\dot{\sigma}_B + \dot{\sigma}_B^2\right)}\dot{\sigma}_A}{\sqrt{2\pi}\left(\dot{\sigma}_A(1-\rho^2) + 4\rho\dot{\sigma}_B\right)}. \tag{11}$$

Substituting (2), (6), (7), and (11)[2] into (8) and performing the necessary mathematical operations, we obtain the LCR of the $\kappa-\mu$ shadowed fading envelope (normalized to the maximum Doppler frequency, f_m) as given in (12), shown at the bottom of the page. For the case when the slopes of the multipath and shadowed components of the received signal are uncorrelated (i.e., $\rho = 0$), (12) can be further reduced to

$$\frac{N_R(r)}{f_m} = \frac{\sqrt{2\pi}\mu^{\mu-\frac{1}{2}} m^{m-\frac{1}{2}} (1+\kappa)^{\mu-\frac{1}{2}} (m+\mu\kappa)^{\frac{1}{2}}}{\Gamma(\mu)(\mu\kappa+m)^m} \left(\frac{r}{\bar{r}}\right)^{2\mu-1} \times \exp\left(-\frac{\mu(1+\kappa)r^2}{\bar{r}^2}\right) {}_1F_1\left(m;\mu;\frac{\mu^2\kappa(1+\kappa)}{\mu\kappa+m}\left(\frac{r}{\bar{r}}\right)^2\right). \tag{13}$$

Fig. 1 shows the shape of the normalized $\kappa-\mu$ shadowed LCR given in (12) for increasing values of m (continuous lines) and

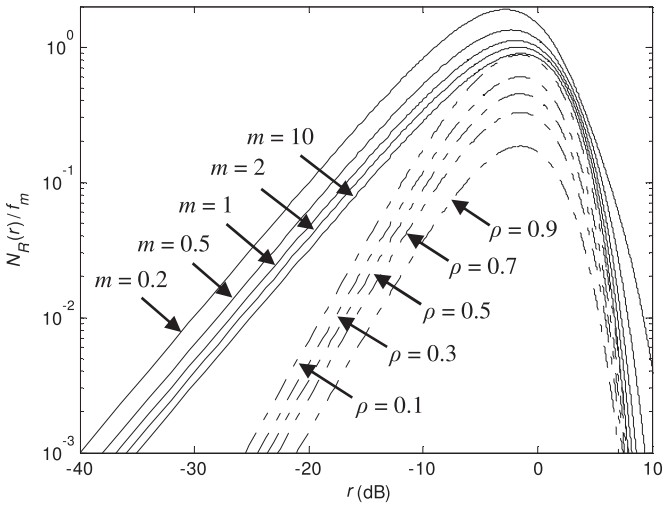

Fig. 1. Normalized LCR for the $\kappa-\mu$ shadowed fading model with decreasing shadowing of the resultant dominant component (continuous lines, $\rho = 0$) and with increasing values of the correlation coefficient (dashed lines, $m = 1$). It should be noted that for all of the plots, $\kappa = 0.5$, $\mu = 2$, and $\bar{r} = 1$.

[2]Equation (6) is used in place of $\dot{\sigma}_A^2$, whereas (7) is used in place of $\dot{\sigma}_B^2$.

$$\frac{N_R(r)}{f_m} = \frac{\sqrt{2\pi(1-\rho^2)}\mu^{\mu-\frac{1}{2}} m^m (1+\kappa)^{\mu-\frac{1}{2}} \left(m+\mu\kappa+2\rho\sqrt{\mu\kappa m}\right)^{\frac{1}{2}}}{\Gamma(\mu)(\mu\kappa+m)^m \left(\sqrt{m}(1-\rho^2)+4\rho\sqrt{\mu\kappa}\right)} \left(\frac{r}{\bar{r}}\right)^{2\mu-1} \exp\left(-\frac{\mu(1+\kappa)r^2}{\bar{r}^2}\right) {}_1F_1\left(m;\mu;\frac{\mu^2\kappa(1+\kappa)}{\mu\kappa+m}\left(\frac{r}{\bar{r}}\right)^2\right) \tag{12}$$

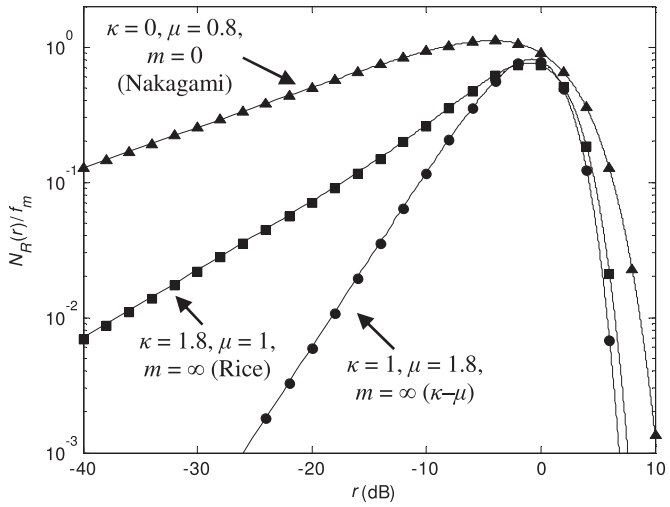

Fig. 2. Normalized LCR for the special cases when the $\kappa - \mu$ shadowed fading model (continuous lines) coincides with the normalized LCR of the Nakagami [15] (triangles), Rice [14] (squares), and $\kappa - \mu$ [17] (circles) models. It should be noted that for all of the plots, $\bar{r} = 1$ and $\rho = 0$ for the $\kappa - \mu$ fading model.

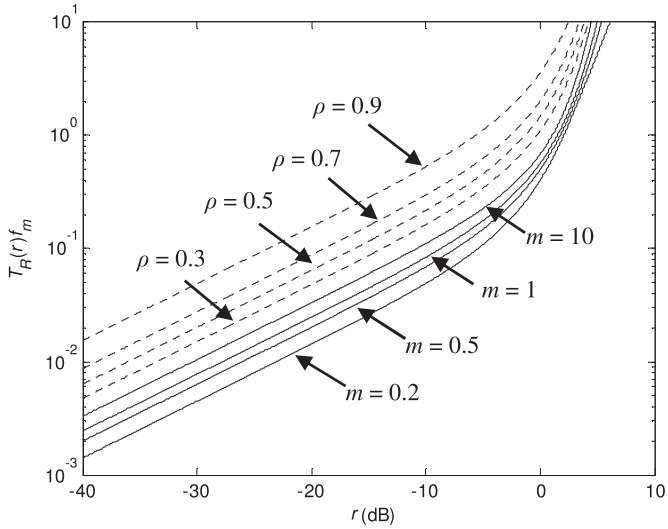

Fig. 3. AFD for the $\kappa - \mu$ shadowed fading model with increasing shadowing of the shadowed dominant component (continuous lines, $\rho = 0$) and with increasing values of the correlation coefficient (dashed lines, $m = 1$). It should be noted that for all of the plots, $\kappa = 0.5$, $\mu = 2$, and $\bar{r} = 1$.

decreasing values of ρ (dashed lines). It is quite evident that as the amount of shadowing of the resultant dominant component decreases, i.e., m gets larger, the signal crosses lower levels at lower rates. Furthermore, the impact of increasing correlation between the slope of the shadowed dominant and multipath signals also acts to cause the signal to cross lower levels at lower rates. Fig. 2 shows the normalized LCR of the $\kappa - \mu$ shadowed fading signal for the special cases when it coincides with the normalized LCRs of the Nakagami [15], Rice [14], and $\kappa - \mu$ [17] fading models, i.e., $\kappa = m = 0$ for Nakagami, $\mu = 1$ and $m = \infty$ for Rice, and $m = \infty$ for $\kappa - \mu$.

IV. Average Fade Duration

The AFD of a fading signal envelope, i.e., $T_R(r)$, is defined as the average length of time that the signal spends below the threshold level R and is related to the LCR through the relationship [15], i.e.,

$$T_R(r) = \frac{F_R(r)}{N_R(r)}. \tag{14}$$

As we can see, to calculate the AFD, it is necessary to have an expression for the cdf, i.e., $F_R(r)$, of the $\kappa - \mu$ shadowed fading signal. As the cdf of the instantaneous SNR in $\kappa - \mu$ shadowed fading channels has been conveniently derived in [1, eq. (6)], to obtain the cdf of the received signal envelope, the same quadratic transformation used to yield the pdf of the fading signal is employed, which gives

$$F_R(r) = \frac{\mu^{\mu-1} m^m (1+\kappa)^\mu}{\Gamma(\mu)(\mu\kappa + m)^m} \left(\frac{r}{\bar{r}}\right)^{2\mu} \times \Phi_2\left(\mu - m, m; \mu + 1; -\frac{\mu(1+\kappa)r^2}{\bar{r}^2}, -\frac{\mu(1+\kappa)m}{(\mu\kappa + m)}\frac{r^2}{\bar{r}^2}\right) \tag{15}$$

where $\Phi_2(\bullet, \bullet; \bullet; \bullet, \bullet)$ is the bivariate confluent hypergeometric function. Now, the normalized AFD of a $\kappa - \mu$ shadowed fading signal can be straightforwardly obtained by substituting (12) and (15) into (14), which gives the equation in (16), shown at the bottom of the page. Again, for the case when the slopes of the multipath and shadowed components of the received signal are uncorrelated (i.e., $\rho = 0$), (16) can be further reduced to (17), shown at the bottom of the page.

Fig. 3 shows the shape of the $\kappa - \mu$ shadowed AFD for increasing values of m (continuous lines) and decreasing values of ρ (dashed lines). As the shadowing of the dominant component decreases, the fading envelope spends more time at lower threshold levels. This is in direct contrast to the correlation between the time derivative of the multipath and shadowed dominant components. In this instance, as the correlation *increases*, the signal can spend more time at lower threshold levels.

$$T_R(r) f_m = \frac{\left(\sqrt{m}(1-\rho^2) + 4\rho\sqrt{\mu\kappa}\right)(1+\kappa)^{\frac{1}{2}}}{\sqrt{2\pi(1-\rho^2)}\,\mu^{\frac{1}{2}}(m + \mu\kappa + 2\rho\sqrt{\mu\kappa m})^{\frac{1}{2}}} \frac{r}{\bar{r}} \Phi_2\left(\mu - m, m; \mu + 1; -\frac{\mu(1+\kappa)r^2}{\bar{r}^2}, -\frac{\mu(1+\kappa)m}{(\mu\kappa+m)}\frac{r^2}{\bar{r}^2}\right) \Big/ \exp\left(-\frac{\mu(1+\kappa)r^2}{\bar{r}^2}\right) {}_1F_1\left(m; \mu; \frac{\mu^2\kappa(1+\kappa)}{\mu\kappa + m}\frac{r^2}{\bar{r}^2}\right) \tag{16}$$

$$T_R(r) f_m = \frac{\sqrt{m}(1+\kappa)^{\frac{1}{2}}}{\sqrt{2\pi}\,\mu^{\frac{1}{2}}(m + \mu\kappa)^{\frac{1}{2}}} \frac{r}{\bar{r}} \Phi_2\left(\mu - m, m; \mu + 1; -\frac{\mu(1+\kappa)r^2}{\bar{r}^2}, -\frac{\mu(1+\kappa)m}{(\mu\kappa+m)}\frac{r^2}{\bar{r}^2}\right) \Big/ \exp\left(-\frac{\mu(1+\kappa)r^2}{\bar{r}^2}\right) {}_1F_1\left(m; \mu; \frac{\mu^2\kappa(1+\kappa)}{\mu\kappa + m}\frac{r^2}{\bar{r}^2}\right) \tag{17}$$

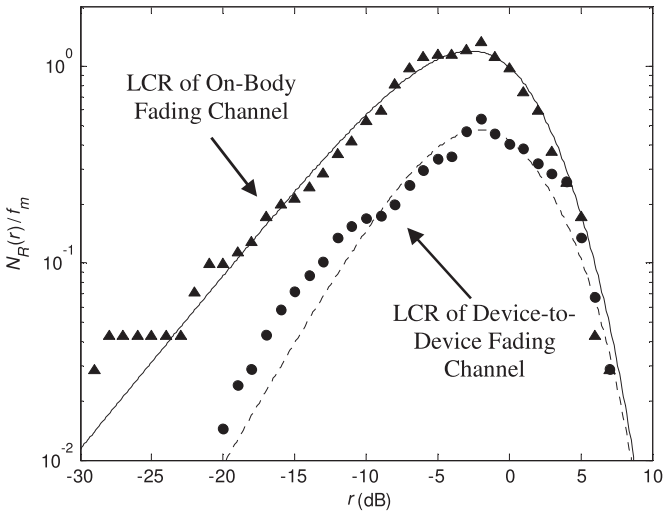

Fig. 4. Comparison of the theoretical (continuous lines) and empirical (shapes) normalized LCRs for the D2D and on-body fading channels. All parameter estimates for the theoretical plots are given in Table I.

V. Comparison With Measured Shadowed Fading Channels

To illustrate the utility of the new equations for modeling shadowed fading channels, they were compared with data obtained from two different sets of field measurements, which considered channels that are known to be susceptible to shadowed fading. The first set of measurements considered cellular D2D communication channels operating at 868 MHz in an outdoor urban environment. Full details of the experimental setup are available in [2] and [18]. This particular scenario considered two persons spaced 10 m apart in an open space between three buildings in a built-up residential area in the suburbs of Belfast in the United Kingdom. Both persons were initially stationary, in direct line-of-sight and had the hypothetical user equipment (UE) positioned at their heads. They were then instructed to move around randomly within a circle of radius 1 m from their starting points while imitating a voice call. The first person's UE was configured to transmit data packets at a power level of 0 dBm with a period of 70 ms for 80 s while the second person's UE recorded the received signal strength indicator of the received packets. The second set of field measurements considered on-body communication channels operating at 2.45 GHz within a highly reverberant environment. Full details of the experimental setup are available in [19]. The on-body link spanned the left-waist to right-knee positions, and the measurements were made when the person performed walking-on-the-spot movements. In this instance, the complex S_{21} was sampled with a period of 5 ms for an interval of 30 s.

Fig. 4 shows the empirical LCRs for both channels compared with the new equation given in (12). All parameter estimates for the $\kappa-\mu$ shadowed fading model were obtained using the `lsqnonlin` function available in the optimization toolbox of MATLAB along with the pdf given in (2). It should be noted that both sets of data were normalized to their respective *rms* signal levels prior to parameter estimation. Using these parameter estimates, the maximum Doppler frequency and correlation were then obtained by minimizing the sum of the squared error between the empirical and theoretical LCR plots. As we can quite clearly see, the normalized LCR of the $\kappa-\mu$ shadowed fading model provides an excellent fit to the on-body data and a very good approximation of the D2D channel.

TABLE I
Estimated Parameters for Measured Shadowed Fading Channels

Fading Channel	$\hat{\kappa}$	$\hat{\mu}$	$\hat{\hat{r}}$	$\hat{m}$	$\hat{f}_m$	$\hat{\rho}$
D2D	1.39	1.78	1.14	0.55	2.40	0.29
On-Body	0.66	1.39	1.03	0.36	4.68	0.05

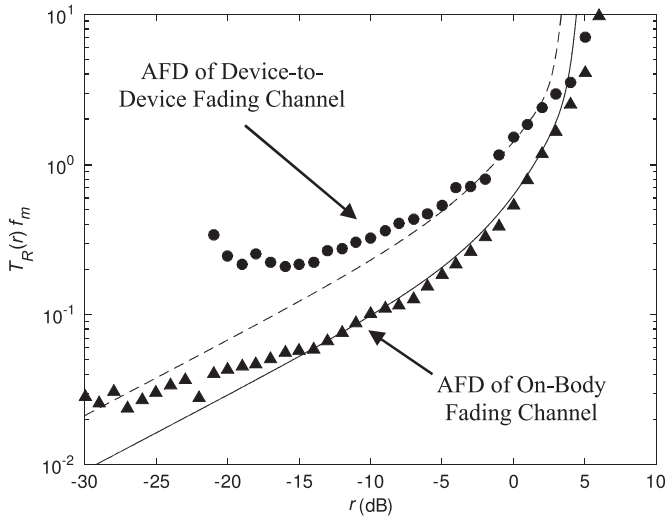

Fig. 5. Comparison of the theoretical (continuous lines) and empirical (shapes) normalized AFDs for the D2D and on-body fading channels. All parameter estimates for the theoretical plots are given in Table I.

To allow the reader to reproduce these plots, parameter estimates for both measurement scenarios are given in Table I. In both applications, it is quite clear that the fading channel is subject to heavy shadowing with $m \leq 0.55$. Furthermore, for the D2D fading channel, it is apparent that the correlation between the slope of the shadowed dominant and multipath components is nonzero. For completeness, Fig. 5 shows both the empirical and theoretical AFD of both types of fading channel. Again, the theoretical AFD provides an excellent representation of the measured data for the on-body fading channel and a good fit for the D2D channel for signal levels above the -10 dB threshold level.

VI. Conclusion

Closed-form expressions for the LCR and AFD of the recently proposed $\kappa-\mu$ shadowed fading model have been presented. These new very general equations will find use in a wide variety of existing and emerging communication applications in which the received signal is subject to shadowed fading, such as D2D communications, body-centric communications, and land mobile satellite communications. The analytical expressions have been validated through reduction to known special cases. It was found that decreasing shadowing of the resultant dominant component reduces crossings at low signal levels but, at the same time, may increase fade durations at these levels. Finally, the utility of the new formulations has been proven through comparison with empirical data obtained for cellular D2D and body-centric fading channels. It has been shown that the second-order statistics of the shadowed fading in both types of channel can be adequately described by the equations proposed here.

ACKNOWLEDGMENT

The author would like to thank the reviewers for their invaluable comments that helped significantly improve the contribution of this work.

REFERENCES

[1] J. F. Paris, "Statistical characterization of $\kappa - \mu$ shadowed fading," *IEEE Trans. Veh. Technol.*, vol. 63, no. 2, pp. 518–526, Feb. 2014.
[2] S. L. Cotton, "Human body shadowing in cellular device-to-device communications: Channel modeling using the shadowed $\kappa - \mu$ fading model," *IEEE J. Sel. Areas Commun.*, vol. 33, no. 1, pp. 111–119, Jan. 2015.
[3] M. D. Yacoub, "The $\kappa - \mu$ distribution and the $\eta - \mu$ distribution," *IEEE Antennas Propag. Mag.*, vol. 49, no. 1, pp. 68–81, Feb. 2007.
[4] M. Nakagami, *The m-Distribution: A General Formula of Intensity Distribution of Rapid Fading, In Statistical Methods in Radio Wave Propagation*. New York, NY, USA: Pergamon, 1960.
[5] A. Abdi, W. C. Lau, M.-S. Alouini, and M. Kaveh, "A new simple model for land mobile satellite channels: First- and second-order statistics," *IEEE Trans. Wireless Commun.*, vol. 2, no. 3, pp. 519–528, May 2003.
[6] J. C. S. S. Filho and M. D. Yacoub, "Nakagami-m approximation to the sum of M non-identical independent Nakagami-m variates," *Electron. Lett.*, vol. 40, no. 15, pp. 951–952, Jul. 2004.
[7] C. Loo, "A statistical model for a land mobile satellite link," *IEEE Trans. Veh. Technol.*, vol. 34, no. 3, pp. 122–127, Aug. 1985.
[8] P. C. Sofotasios and S. Freear, "On the $\kappa - \mu$/gamma composite distribution: A generalized multipath/shadowing fading model," in *Proc. SBMO/IEEE MTT-S Int. Microw. Optoelectron. Conf.*, Oct. 2011, pp. 390–394.
[9] S. R. Panic *et al.*, "Second-order statistics of selection macro-diversity system operating over gamma shadowed—Fading channels," *Eurasip J. Wireless Commun. Netw.*, p. 155, 2011.
[10] N. Youssef, T. Munakata, and M. Takeda, "Fade statistics in Nakagami fading environments," in *Proc. IEEE 4th Int. Symp. Spread Spectrum Techn. Appl.*, Sep. 1996, vol. 3, pp. 1244–1247.
[11] S. L. Cotton, "A statistical model for shadowed body-centric communications channels: Theory and validation," *IEEE Trans. Antennas Propag.*, vol. 62, no. 3, pp. 1416–1424, Mar. 2014.
[12] J. Abad and J. Sesma, "Computation of the regular confluent hypergeometric function," *Mathematica J.*, vol. 5, no. 4, pp. 74–76, 1995.
[13] S. O. Rice, "Statistical properties of a sine wave plus random noise," *Bell Syst. Tech. J.*, vol. 27, no. 1, pp. 109–157, Jan. 1948.
[14] G. L. Stuber, *Principles of Mobile Communication*, 3rd ed. New York, NY, USA: Springer-Verlag, 2011.
[15] M. D. Yacoub, J. E. V. Bautista, and L. Guerra de Rezende Guedes, "On higher order statistics of the Nakagami-m distribution," *IEEE Trans. Veh. Technol.*, vol. 48, no. 3, pp. 790–794, May 1999.
[16] A. Papoulis, *Probability, Random Variables, and Stochastic Processes*, 3rd ed. New York, NY, USA: McGraw-Hill, 1991.
[17] S. L. Cotton and W. G. Scanlon, "Higher-order statistics for $\kappa - \mu$ distribution," *Electron. Lett.*, vol. 43, no. 22, pp. 1215–1217, Oct. 2007.
[18] S. L. Cotton, "Channel measurements of device-to-device communications in an urban outdoor environment," in *Proc. XXXIth URSI GASS*, Aug. 2014, pp. 1–4.
[19] S. L. Cotton, "A statistical characterization of on-body fading using the shadowed $\kappa - \mu$ fading model," in *Proc. IEEE APSURSI*, Jul. 2014, pp. 717–718.

Exploiting Macrodiversity in Massively Distributed Antenna Systems: A Controllable Coordination Perspective

Wei Feng, *Member, IEEE*, Yunfei Chen, *Senior Member, IEEE*, Rui Shi, Ning Ge, *Member, IEEE*, and Jianhua Lu, *Fellow, IEEE*

***Abstract*—The massively distributed antenna system (MDAS) can offer a significant macrodiversity gain in comparison with traditional colocated massive multiple-input multiple-output (MIMO). Thus, it is a promising candidate for future network densification. Coordinated antenna selection (CAS), by harmoniously activating a subset of the antennas, can efficiently exploit the benefit of MDAS while reducing the number of radio-frequency chains. However, perfect CAS usually requires global channel state information (CSI), which consequently leads to a tremendous amount of system overhead. To control the cost of CAS, in this paper, we propose the use of *visible antennas* (VAs) for each mobile terminal (MT). Assuming that only the CSI between a given MT and its VAs is acquired, we use the number of VAs to quantitatively characterize a general partial-CSI condition. Then, we formulate the corresponding CAS problem as a nonconvex integer programming problem. By adopting variable relaxation and successive approximation, we derive a suboptimal solution to the problem based on geometric programming. Simulation results illustrate that the proposed CAS scheme can offer a near-optimal performance gain in terms of achievable sum rate for any randomly chosen number of VAs.**

***Index Terms*—Controllable coordination, coordinated antenna selection (CAS), geometric programming (GP), massively distributed antenna system (MDAS), visible antenna (VA).**

I. INTRODUCTION

Recently, network densification by deploying more antenna elements [1] or more sites, such as relaying nodes [2], has been considered as an effective means of capacity improvement. In particular, it is widely recognized that deploying the antenna elements in a distributed manner, thus forming a massively distributed antenna system (MDAS) [3], may achieve a dramatic capacity gain over the colocated case, due to reduced access distance and increased macrodiversity [4]–[6].

Coordinated antenna selection (CAS) that jointly activates a subset of the distributed antennas for multiple mobile terminals (MTs) can exploit the macrodiversity of DAS while reducing the number of radio-frequency chains. In [7], the selective transmission (ST) scheme, where an MT is served by the nearest antenna, was proposed. Considering user fairness, Ahmad *et al.* in [8] further put forward a coordinated antenna-port selection and beamforming scheme. All

Manuscript received May 20, 2015; revised September 13, 2015, November 28, 2015; accepted December 3, 2015. Date of publication December 8, 2015; date of current version October 13, 2016. This work was supported in part by the National Science Foundation of China under Grant 61201186, by the National Basic Research Program of China under Grant 2013CB329001, and by the National Science Foundation of China under Grant 61321061 and Grant 61271265. The review of this paper was coordinated by Prof. D. B. da Costa.

W. Feng, N. Ge, and J. Lu are with the Tsinghua National Laboratory for Information Science and Technology, Tsinghua University, Beijing 100084, China (e-mail: fengw@mails.tsinghua.edu.cn; gening@tsinghua.edu.cn; lhhdee@tsinghua.edu.cn).

Y. Chen is with the School of Engineering, University of Warwick, Coventry CV4 7AL, U. K. (e-mail: Yunfei.Chen@warwick.ac.uk).

R. Shi is with the School of Aerospace Engineering, Tsinghua University, Beijing 100084, China (e-mail: r.shi@mail.tsinghua.edu.cn).

Color versions of one or more of the figures in this paper are available online at http://ieeexplore.ieee.org.

Digital Object Identifier 10.1109/TVT.2015.2506720